

Coarse scale representation of spiking neural networks: backpropagation through spikes and application to neuromorphic hardware

Angel Yanguas-Gil

Applied Materials Division, Argonne National Laboratory

Lemont, Illinois

ayg@anl.gov

ABSTRACT

In this work we explore recurrent representations of leaky integrate and fire neurons operating at a timescale equal to their absolute refractory period. Our coarse time scale approximation is obtained using a probability distribution function for spike arrivals that is homogeneously distributed over this time interval. This leads to a discrete representation that exhibits the same dynamics as the continuous model, enabling efficient large scale simulations and backpropagation through the recurrent implementation. We use this approach to explore the training of deep spiking neural networks including convolutional, all-to-all connectivity, and maxpool layers directly in Pytorch. We found that the recurrent model leads to high classification accuracy using just 4-long spike trains during training. We also observed a good transfer back to continuous implementations of leaky integrate and fire neurons. Finally, we applied this approach to some of the standard control problems as a first step to explore reinforcement learning using neuromorphic chips.

CCS CONCEPTS

• **Computing methodologies** → **Neural networks**; *Machine learning*.

KEYWORDS

spiking neurons, neural networks, neuromorphic computing, machine learning

1 INTRODUCTION

Spiking neurons have long been the subject of intense study due to their central role in the central nervous system. Recently, there has been a renewed interest in the subject in the context of artificial intelligence and neuromorphic hardware, where spiking neurons offer the promise of power-efficient computing architectures capable of tackling problems that are hard to solve using conventional computational approaches.

One of the fundamental challenges of using spiking neurons for computations or machine learning applications is how to adapt the stochastic gradient descent methods at the core of training algorithms for artificial neural networks to their spiking counterparts. The motivation for doing so is twofold: first, it provides a way of implementing machine learning algorithms in neuromorphic hardware. Second, it facilitates the use of existing machine learning tools to explore the computational capabilities of biological neural networks.

Not surprisingly, this is a problem that has been repeatedly tackled in the literature. The proposed approaches can be split into two broad categories: one type of approach has focused on how to efficiently transfer trained networks from artificial neural networks to their spiking counterparts. The second type of approach explores heuristic approximations for gradients or algorithms in spiking networks themselves. Both have yielded promising results.[2, 4, 5, 7–9]

In this work, we explore the connection between piece-wise differentiable continuous models of spiking neurons and recurrent neural networks. Our motivation is that, from a machine learning perspective, modeling spiking neurons is very inefficient: the time scale used in the discretization of the differential equations controlling the neuron dynamics is typically much smaller than the timescales at which information propagates through the network. If we find coarse-scale models that evolve at a faster pace, we can 1) efficiently implement larger networks 2) minimize the number of timesteps required when training spiking neural networks using stochastic gradient descent methods.

In particular, we exploit the presence of an absolute refractory period defining the largest timescale at which a neuron can spike *at most once*. A model that is capable of evolving at this pace while reproducing the underlying dynamics of the spiking neuron would provide a very efficient implementation. The existence of such system is however by no means guaranteed: there is no one-to-one correlation between a system of differential equations and a discrete implementation with arbitrarily large time steps.

In this work, we therefore seek to understand how we can create coarse-scale approximations of spiking systems that allow us to map spiking models into recurrent systems that evolve at time scales of the order of the absolute refractory period of neurons. Our approach is based on managing the loss of information on the exact timings of the system at timescales smaller than our evolution step by transforming the differential equations of leaky integrate and fire (LIF) neurons into a probabilistic models. By making fundamental assumptions about the distributions characterizing spike arrival and spike generation we can derive different coarse-scale models.

This paper is structured as follows: we first derive three different coarse-scale models from a standard leaky integrate and fire equations. We then benchmark these models against the LIF neurons by exploring sparsely connected spiking neurons. After demonstrating the equivalence of some of these models, we implement stochastic gradient descent methods and explore the training of shallow and deep spiking neural networks using this approach. Finally, we explore the use of spiking networks for control tasks as a first step for their implementation in neuromorphic hardware.

2 MODEL

This work uses the leaky integrate and fire neuron as a model system for spiking neurons. In a LIF model, the membrane potential v_i of the neuron is given by:

$$\tau \frac{dv_i}{dt} = -v_i + \tau \sum_j w_{ij} \delta(t - t_{ij}) + \tau u_{\text{ext}}^{(i)} \quad (1)$$

Here spikes are treated as Dirac's delta impulses, w_{ij} are the synaptic weights, and τ is the leakage time of the membrane potential of the neuron, and $u_{\text{ext}}^{(i)}$ is a term comprising non-spiking external currents. Each neuron is subject to the spike firing condition whenever the membrane potential reaches a threshold value $v_0^{(i)}$:

$$v_i(t) = v_0^{(i)} \Rightarrow v_i(t + t') = 0 \quad \forall \quad t' < \tau_r \quad (2)$$

For simplicity, we have chosen a reset potential $v_{\text{reset}} = 0$, but generalizations to other values are straightforward. The key parameter of the model is the absolute refractory period τ_r , defining the time after a spike during which the membrane potential is not receptive towards incoming input. This absolute refractory period provides the coarsest timescale during which each neurons spikes at most once. It is therefore the natural timescale that we can use to build an efficient coarse-scale representation of this type of neurons.

Eq. 1 can be integrated over a timescale Δt to obtain:

$$v_i(t + \Delta t) = v_i(t) e^{-\Delta t/\tau} + \tau u_{\text{ext}}^{(i)} \left(1 - e^{-\Delta t/\tau}\right) + \sum_{j:t_{ij} < t + \Delta t} w_{ji} e^{-(t + \Delta t - t_{ij})/\tau} \quad (3)$$

where the sum is extended to all spikes received within the t and $t + \Delta t$ interval. Here we have assumed that $u_{\text{ext}}^{(i)}$ change slowly during that interval.

As we move to a coarse scale representation we lose information on the exact firing times Δt . Therefore, we assume that the actual spike arrival times t_{ij} are homogeneously distributed between t and $t + \Delta t$ with a probability density $1/\Delta t$. This leads to the following averaged contribution of incoming spikes to Eq. 3:

$$\langle e^{-(t + \Delta t - t_{ij})/\tau} \rangle = \frac{1}{\Delta t} \int_t^{t + \Delta t} e^{-(t + \Delta t - t_{ij})/\tau} dt_{ij} = \frac{\tau}{\Delta t} \left(1 - e^{-\Delta t/\tau}\right) \quad (4)$$

For the specific case of $\Delta t = \tau_r$, and defining $s_i = 0, 1$ depending on whether the neuron spikes in each interval, we have that:

$$v_i(n) = v_i(n-1) e^{-\tau_r/\tau} + \xi_i(n) \left(1 - e^{-\tau_r/\tau}\right) \quad (5)$$

and

$$\xi_i(n) = \tau u_{\text{ext}}^{(i)}(n) + \frac{\tau}{\tau_r} \sum_j w_{ij} s_j(n - n_{ij}) \quad (6)$$

where

$$s_i(n) = H\left(v_i(n) - v_0^{(i)}\right) \quad (7)$$

where $H(\cdot)$ is the Heaviside or step function and $v_0^{(i)}$ is the firing threshold.

Eq. 5 assumes that the neuron did not fire in the prior interval. If a neuron spiked in the past interval we need to account for the refractory period, during which the voltage is assumed to be clamped to its reset value. Depending on the assumption that we make about when a neuron spikes, we can define three different models:

2.1 Model I

Model I assumes that the precise instant in which the neuron leaves its refractory period is uniformly distributed over $\Delta t = \tau_r$. This means that the neuron will be receptive to external inputs only during a fraction δt within the interval Δt , so that:

$$v_i(t + \delta t) = v_{\text{ext}}^{(i)} \left(1 - e^{-\delta t/\tau}\right) + \sum_{j:t_{ij} < t + \delta t} w_{ji} e^{-(\delta t - t_{ij})/\tau} \quad (8)$$

we then have to average over t_{ij} and δt to obtain:

$$v_i(n) = \xi_i(n) \left(1 - \frac{\tau}{\Delta t} (1 - e^{-\Delta t/\tau})\right) \quad (9)$$

If we now particularize $\Delta t = \tau_r$, we have replaced the asynchronous leaky integrate and fire model with a recurrent discrete time difference equations that neglects timescales smaller than the absolute refractory period of the networks.

Eqs. 5 and 9 can be concisely expressed as:

$$v_i(n) = (1 - s_i(n-1)) \left[v_i(n-1) e^{-\tau_r/\tau} + \xi_i(n) \left(1 - e^{-\tau_r/\tau}\right) \right] + s_i(n-1) \xi_i(n) \left(1 - \frac{\tau}{\tau_r} (1 - e^{-\tau_r/\tau})\right) \quad (10)$$

2.2 Model II

Model II considers that the neuron fires at the end of the time interval, clamping the potential to its reset value during the next step. Consequently, while neurons in Model I can spike during each interval, in Model II neurons can spike at most once every two intervals.

The resulting recurrent expression for this model is therefore:

$$v_i(n) = (1 - s_i(n-1)) \left[v_i(n-1) e^{-\tau_r/\tau} + \xi_i(n) \left(1 - e^{-\tau_r/\tau}\right) \right] \quad (11)$$

2.3 Model III

Model III resets the potential but otherwise the system is receptive to spikes during the next interval after the neuron spikes:

$$v_i(n) = (1 - s_i(n-1)) v_i(n-1) e^{-\tau_r/\tau} + \xi_i(n) \left(1 - e^{-\tau_r/\tau}\right) \quad (12)$$

In all three cases, $s_i(n) = H\left(v_i(n) - v_0^{(i)}\right)$.

3 VALIDATION OF THE COARSE-SCALE APPROXIMATION

To validate the accuracy of the three models, we have compared their performance with their corresponding asynchronous leaky integrate and fire. We have considered a network of 1000 randomly connected neurons with a connectivity density of 5%. This type of networks has been well characterized in the literature, and it is characterized by a complex dynamics. It is therefore the perfect model to explore the impact of the coarse scale models.

Here we consider the case in which neurons are excited with constant external inputs sampled from a Gaussian distribution. In Figure 1 we show the Pearson correlation between the average activities of the LIF models and the three discrete approximations. Each point corresponds to a different network randomly instantiated and with randomly selected inputs. Results are shown for three values of τ/τ_r .

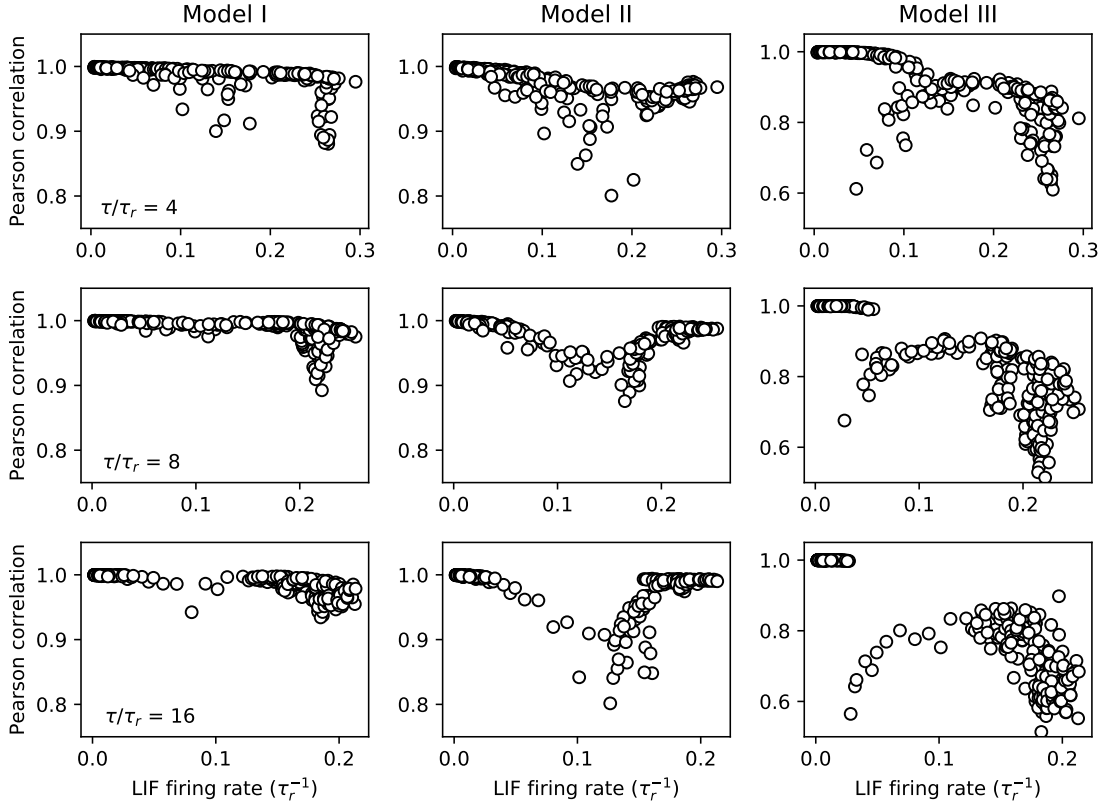


Figure 1: Pearson correlation between the firing rates (spikes per unit time) of the asynchronous LIF and the synchronous representation for $\Delta t = \tau_r$ as a function of the average activity of the network. Results are shown for Models I, II, and III, and three values of τ/τ_r . The loss of information on the exact spiking times has only marginal effects for Models I and II the activity is low.

Despite the loss of information on the timing of spikes at timescales shorter than the absolute refractory period, the results indicate a good agreement between the average activity of Model I and the LIF model. Model II has also a reasonably good agreement. However, Model III fails to reproduce the dynamics of the recurrent LIF network (note the different vertical scale for the correlation in Figure 1). This emphasizes the importance of managing the information about spike timings that is lost when shifting to coarser time scales.

4 STOCHASTIC GRADIENT DESCENT IMPLEMENTATION

After validating that Model I and Model II agree reasonably well with the LIF model, the implemented stochastic gradient descent methods in these two models. Both Eq. 10 and 11 allow us to represent a spiking network as a recurrent layer of the output spike s and the membrane potential v , so that:

$$s(t), v(t) = f(\xi(t); s(t-1), v(t-1)) \quad (13)$$

where s and v are related through:

$$s = H(v - v_0) \quad (14)$$

In order to enable stochastic gradient descent methods, we calculate s using Eq. 14 in the forward direction, whereas in the backward direction gradients are calculated using a differentiable approximation. Here, we have used the logistic function $\sigma(\cdot)$, so that:

$$s_{\text{back}} = \sigma(\beta(v - v_0)) \quad (15)$$

Here β is a regularization parameter that determines the steepness of the approximation. In this work, we implemented these models directly in Pytorch. Details on the implementation are included in the Appendix, and the code can be found online at: <https://github.com/anglyan/spikingtorch>.

While Eq. 13 allows us to train networks to match specific spike trains, here we have considered the total activity of the output neurons:

$$a = \sum_t s(t) \quad (16)$$

This would in principle allow us to consider two different approaches: we can try to match a specific number of spikes N_{out} , or we can use a cross-entropy cross-section that tries to maximize the activity of specific neurons. Our experience shows that cost

functions such as MSE that take into account the number of output spikes perform more consistently than the cross-entropy method.

In our recurrent implementation of spiking neurons, inputs and outputs are codified as a time sequence of length N_{sp} . We have considered the following four type of encodings:

- (1) *random spike train*. Input values are codified as a Bernoulli distribution, the discrete equivalent of Poisson spike trains.
- (2) *Periodic spike train*. A periodic train of spikes spaced by an interval that is inversely related to the intensity of the input.
- (3) *Single spike delay encoding*. In this case the input is codified as a single spike whose delay with respect to a common epoch decreases with the input intensity.
- (4) *Constant analog input*. The input is codified as constant input signal.

5 RESULTS

5.1 Shallow and multilayer spiking networks

In order to test the proposed approach we first tested its performance in classification tasks involving the MNIST and Fashion MNIST datasets.[6, 10]. We considered the following networks:

- **Shallow network**: input spikes are densely connected to the output neurons with no bias.
- **In/Lin/Sp/Lin/Sp**: a densely connected network with one hidden layer of spiking neurons. The results shown in this work have been obtained using 30 hidden neurons.
- **In/Conv/Sp/Lin/Sp**: a simple convolutional network with a 2D convolutional layer composed of a 5x5 kernel with a stride and padding of 2 outputting to four independent channels. This results on 784 spiking neurons that are then fully connected to the spiking output layer through a linear layer with no bias.
- **In/Conv/Sp/Conv/Sp/Lin/Sp**: a convolutional network with two 2D convolutional layers, each with a 5x5 kernel. The first layer, with the same configuration as the single layer case, has a stride and padding of 2 outputting to four independent channels. The second convolutional layer has a stride of 1 and 6 output channels. The output is then fed to a spiking layer that is fully connected to the spiking output layer with no bias.

The additional case of a spiking LeNet5 is analyzed in Section 5.3.

These networks, implemented using Model I, were trained against the MNIST and Fashion MNIST (FMNIST) datasets, resulting on the classification accuracy values shown in Table 1. These results were obtained for an 8-long spike trains trained for 15 epochs with a MSE cost function and a desired activation pattern of the output layers of 4 spikes for the correct neuron. The threshold voltage was kept constant and equal to $v_0^i = 1$. In Table 1 we also show the comparison with two separate benchmarks: in the first benchmark, the spiking layers were replaced with rectified linear units except for the output layer, where a softmax function is used. This first benchmark was trained using a cross-entropy loss function. The second benchmark replaced all spiking neurons with sigmoid layers, and the training is carried out using an MSE cost function, the same as the spiking case. A third benchmark in which all neurons

are replaced with rectified linear units was briefly considered, but it failed to achieve good classification accuracies in FMNIST.

In all cases, the stochastic gradient descent method was able to converge to an accuracy comparable to that of the non-spiking counterpart, demonstrating the ability to carry out backpropagation both through the depth of the network and through spike trains. Access to efficient implementations of convolutional layers and GPU compatibility greatly aided the computational efficiency of the training process, resulting on a significant acceleration compared to CPU-based approaches. Moreover, a comparison between the two benchmarks shows that sigmoidal activation functions lead to lower accuracies compared to the ReLU benchmark. This may suggest that the bounded nature of the output of spiking neurons, together with smaller gradients far from the firing threshold, could account for the small dip in accuracy with respect to the ReLU benchmark.

5.2 Analysis of the shallow network case

We have used the shallow network case to look more in depth to some of the particularities of the recurrent models used in this work.

First, we have looked at the transfer of trained recurrent networks to the conventional LIF model represented by the differential Eq. 1. This is something that is relevant, for instance, if we want to transfer trained networks to neuromorphic hardware or to a software model providing an exact implementation of LIF neurons.

In Figure 2 we show the accuracy achieved by a simple shallow spiking network of Models I and II, and we compare it with the resulting efficiency when the same network is transferred back to the fine-scale LIF model where spikes are treated as Dirac's delta functions. We observe an excellent correlation between the classification accuracy obtained in the coarse scale and in the LIF models.

Then we explored the impact that the number of target output neurons spikes N_{out} used during training had on the network accuracy. As shown in Figure 2, there is a minimum number of output spikes required in order to achieve the maximum accuracy. For 8-long spike trains we need to require at least four output spikes in the correct output neuron for the algorithm to effectively carry out the classification task. This is observed for both Model I and Model II.

Finally, we explored the impact that the slope parameter β used in the regularization of the Heaviside function (Eq. 15 has on the ability to classify both datasets. As shown in Table 2, there is a small dependence with β , with both classification accuracy and the agreement between the coarse-scale and the LIF model being slightly better for $\beta \geq 3$.

5.3 Spiking LeNet5

To deepen our understanding of the design principles of deep spiking networks we have focused on a spiking version of the LeNet5 network.[6] The spiking version of this network maintains the convolutional and maxpool layers of the non-spiking version and replaces the five non-linear layers with spiking neuron counterparts.

Table 1: Classification accuracy of trained spiking networks based on Model I for 8-long Bernoulli input spike trains. Two non-spiking benchmarks are shown for comparison: one where inner spiking layers are replaced with rectified linear units and the output with a softmax, and a second case where all spiking layers were replaced with sigmoid activation functions. All cases were trained for 15 epochs

Network	Spiking		ReLU+SoftMax		Sigmoid	
	MNIST	FMNIST	MNIST	FMNIST	MNIST	FMNIST
Shallow	91.0	81.4	92.9	84.1	92.0	83.7
In/Lin/Sp/Lin/Sp	95.6	84.7	96.8	86.6	95.0	86.4
In/Conv/Sp/Lin/Sp	96.4	84.9	97.6	87.3	97.0	86.6
In/Conv/Sp/Conv/Sp/Lin/Sp	97.9	85.7	98.4	87.8	97.8	86.3

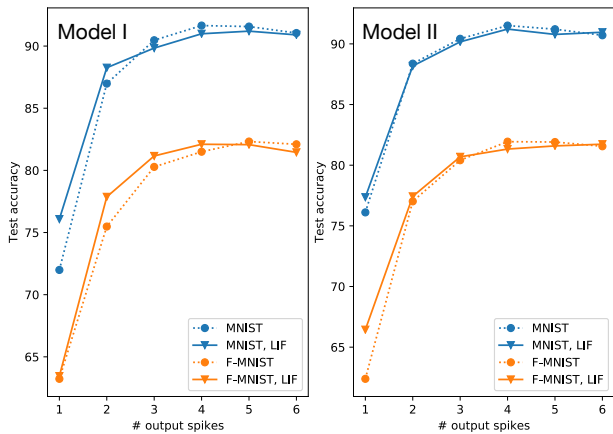


Figure 2: accuracy of a shallow spiking network implementing Model I (left) and Model II (right) in MNIST and Fashion MNIST classification tasks. The accuracy of the coarse-scale model and that of the full LIF model on the trained network is shown as a function of the number of spikes used in the training process.

Table 2: Impact of the slope parameter β controlling spike regularization on the classification accuracy of both MNIST and Fashion MNIST in a shallow network

	Value of β				
	1	2	3	4	5
MNIST	90.6	91.0	91.0	90.9	90.7
FMNIST	79.7	80.7	81.4	81.7	81.8

Here we have compared two different encodings: a random spike train, based on a Bernoulli distribution with an average equal to the pixel intensity, and a periodic spike train. For the periodic spike train cases we added a sixth layer of spiking neurons where the pixel intensities, normalized from 0 to 1, are transformed into a periodic train of spikes, mimicking the behavior of sensory neurons.

Table 3: Classification accuracy of spiking LeNet network for 8-long spike trains. All cases were trained during 15 epochs using the same training conditions.

Encoding	Bias	MNIST	FMNIST
Poisson	yes	98.8	87.5
Periodic	yes	98.6	88.0
Poisson	no	98.6	87.5
Periodic	no	98.6	87.4
Benchmarks			
ReLU + SoftMax	yes	98.8	90.3
ReLU + SoftMax	no	99.0	89.6
Sigmoid	yes	98.8	89.5
Sigmoid	no	98.8	88.4

The rest of the network remains the same. We have also compared the case where biases are omitted from the three densely connected layers in LeNet5. This is consistent with the presence of a constant firing threshold for all the neurons in the network.

In Table 3 we show a comparison between these four cases for the MNIST and F-MNIST datasets. We have considered the same two benchmarks used in Section 5.1. We report top-one accuracy values in all cases. The results obtained are remarkable insensitive towards the type of encoding. This is somewhat unexpected given the dependence on accuracy with spike length reported in other methods, which required up to 150 steps for the more complex networks. Also, the presence of additional bias in the fully connected layers do not seem to greatly impact the network’s accuracy. It is feasible that some of these differences could be fleshed out with different training strategies or by training for a considerable larger number of epochs.

Finally, in order to evaluate the impact of the length of the spike trains used during training, we performed an experiment where networks trained with random spike trains of a given length were then tested using spike trains of varying lengths. The results, summarized in Table 4, show how networks trained with as few as 4-long spike trains can be successfully transferred during inference to inputs with longer spike trains, resulting on higher classification accuracy. Still, it is important to note that the difference in accuracy for short and long spike trains is small, ranging between 0.5 and 1%.

Table 4: Impact of spike train length during training and testing in spiking LeNet’s accuracy on MNIST. Values are the average of ten independent tests, with the standard deviation in the second decimal place.

Input length	Testing						
Training	4	6	8	12	16	32	48
4	98.52	98.82	98.91	98.98	99.00	99.02	99.00
6	98.48	98.82	98.90	98.96	98.99	99.03	99.03
8	98.43	98.81	98.90	98.97	98.97	99.01	99.00
12	98.21	98.70	98.85	98.95	99.00	99.07	99.10

5.4 Application to neuromorphic hardware and control tasks

As shown in a previous work, our implementation of the LIF model provides an excellent agreement with the fixed-point implementation in Loihi.[3, 12] Therefore, we can directly use these models to train and port spiking neural network into neuromorphic hardware. We have also applied this model to explore the optimization of neuromorphic architectures implemented using cross-point arrays.[11]

In order to evaluate the feasibility of training LIF neurons directly using backpropagation for control tasks, we have explored their application to standard reinforcement learning benchmarks such as Cartpole.[1] We have considered a spiking neural network in which the four-dimensional inputs from the environment are passed through a densely connected linear layer into a hidden layer of spiking neurons, which are in turn densely connected to the two output spiking neurons.

The output layer accumulates the number of spikes \mathbf{n}_s over a finite number of steps N_{sp} , and transforms it into a value that can be directly used to calculate the response probabilities:

$$\mathbf{y} = \sigma \left[\alpha \left(\mathbf{n}_s - \frac{N_{sp}}{2} \right) \right] \quad (17)$$

where α is a scaling parameter used to ensure that \mathbf{y} covers a sufficiently large fraction of the $[0, 1]$ interval.

We have used a naive implementation of the cross-entropy algorithm to dynamically learn the optimal policy by training the network using the upper 30% percentile of episodes in each batch. For a hidden layer of 64 neurons we can achieve an average of 199.3 steps over 100 consecutive episodes with 8-long spike trains using fewer than 50 batches of 32 episodes.

6 CONCLUSIONS

In this work we have explored recurrent representations of leaky integrate and fire neurons operating at a timescale equal to their absolute refractory period. This leads to highly efficient implementations that present identical dynamics, which provides unique opportunities for large scale simulations and the efficient emulation of existing neuromorphic hardware implementing leaky integrate and fire neurons.

The exploration of coarse-scale representation of leaky integrate and fire networks leads to a straightforward implementation of stochastic gradient descent method in spiking neurons without the need of approximating the gradients beyond the regularization of a step-function during the backward step. We have explored the application of this methodology to networks with up to six layers

of spiking neurons, and we have shown that training a spiking LeNet5 network with 4-long spike trains is enough to achieve 99% accuracy in the MNIST task. Likewise, we have demonstrated that 8-long spike trains are enough to train a spiking network on the Cartpole task using the same backpropagation methods.

The approach outlined in this work provides a straightforward entry point to explore the potential of spiking networks using conventional machine learning frameworks.

ACKNOWLEDGMENTS

This research is based upon work supported by Laboratory Directed Research and Development (LDRD) funding from Argonne National Laboratory, provided by the Director, Office of Science, of the U.S. Department of Energy under Contract No. DE-AC02-06CH11357.

REFERENCES

- [1] A. G. Barto, R. S. Sutton, and C. W. Anderson. 1983. Neuronlike adaptive elements that can solve difficult learning control problems. *IEEE Transactions on Systems, Man, and Cybernetics* SMC-13, 5 (1983), 834–846.
- [2] Sander M. Bohte, Joost N. Kok, and Han [La PoutrĀĈĀ]. 2002. Error-backpropagation in temporally encoded networks of spiking neurons. *Neurocomputing* 48, 1 (2002), 17 – 37. [https://doi.org/10.1016/S0925-2312\(01\)00658-0](https://doi.org/10.1016/S0925-2312(01)00658-0)
- [3] M. Davies, N. Srinivasa, T. Lin, G. Chinya, Y. Cao, S. H. Choday, G. Dimou, P. Joshi, N. Imam, S. Jain, Y. Liao, C. Lin, A. Lines, R. Liu, D. Mathaikutty, S. McCoy, A. Paul, J. Tse, G. Venkataramanan, Y. Weng, A. Wild, Y. Yang, and H. Wang. 2018. Loihi: A Neuromorphic Manycore Processor with On-Chip Learning. *IEEE Micro* 38, 1 (2018), 82–99.
- [4] Peter U. Diehl, Guido Zarrrella, Andrew Cassidy, Bruno U. Pedroni, and Emre Neftci. 2016. Conversion of Artificial Recurrent Neural Networks to Spiking Neural Networks for Low-power Neuromorphic Hardware. arXiv:1601.04187 [cs.NE]
- [5] Eric Hunsberger and Chris Eliasmith. 2015. Spiking Deep Networks with LIF Neurons. arXiv:1510.08829 [cs.LG]
- [6] Y. Lecun, L. Bottou, Y. Bengio, and P. Haffner. 1998. Gradient-based learning applied to document recognition. *Proc. IEEE* 86, 11 (1998), 2278–2324.
- [7] Chankyu Lee, Syed Shakib Sarwar, Priyadarshini Panda, Gopalakrishnan Srinivasan, and Kaushik Roy. 2020. Enabling Spike-Based Backpropagation for Training Deep Neural Network Architectures. *Frontiers in Neuroscience* 14 (2020), 119. <https://doi.org/10.3389/fnins.2020.00119>
- [8] Jun Haeng Lee, Tobi Delbruck, and Michael Pfeiffer. 2016. Training Deep Spiking Neural Networks Using Backpropagation. *Frontiers in Neuroscience* 10 (2016), 508. <https://doi.org/10.3389/fnins.2016.00508>
- [9] Abhronil Sengupta, Yuting Ye, Robert Wang, Chiao Liu, and Kaushik Roy. 2019. Going Deeper in Spiking Neural Networks: VGG and Residual Architectures. *Frontiers in Neuroscience* 13 (2019), 95. <https://doi.org/10.3389/fnins.2019.00095>
- [10] Han Xiao, Kashif Rasul, and Roland Vollgraf. 2017. Fashion-MNIST: a Novel Image Dataset for Benchmarking Machine Learning Algorithms. arXiv:1708.07747 [cs.LG]
- [11] Angel Yanguas-Gil. 2019. Memristor design rules for dynamic learning and edge processing applications. *APL Materials* 7, 9 (2019), 091102. <https://doi.org/10.1063/1.5109910> arXiv:https://doi.org/10.1063/1.5109910
- [12] A. Yanguas-Gil, A. Mane, J. W. Elam, F. Wang, W. Severa, A. R. Daram, and D. Kudithipudi. 2019. The Insect Brain as a Model System for Low Power Electronics and Edge Processing Applications. In *2019 IEEE Space Computing Conference (SCC)*. 60–66.

A IMPLEMENTATION DETAILS

The implementation of stochastic gradient descent methods using the coarse scale representation derived in this work requires the propagation of gradients over Heaviside functions using a differentiable approximation. The implementation of this function in a machine learning framework such as Pytorch is straightforward:

```
class HardSoft(torch.autograd.Function):  
  
    @staticmethod  
    def forward(ctx, input, constant):  
        ctx.constant = constant  
        output = torch.sigmoid(constant*input)  
        ctx.save_for_backward(output)
```

```
        return H(input)  
  
    @staticmethod  
    def backward(ctx, grad_output):  
        out, = ctx.saved_tensors  
        return grad_output * out*(1-out)*ctx.constant, None  
  
def H(x):  
    return 0.5*(torch.sign(x)+1)
```

The rest of the algorithms can be implemented using the standard methods as described in Pytorch's documentation. The code used to compute some of the examples in this work can be found in the following website: <https://github.com/anglyan/spikingtorch>.